OXFORD

ORIGINAL ARTICLE

Structural and Maturational Covariance in Early Childhood Brain Development

Xiujuan Geng[1,4,6], Gang Li[2], Zhaohua Lu[5], Wei Gao[3], Li Wang[2],
Dinggang Shen[2,7], Hongtu Zhu[5] and John H. Gilmore[1]

[1]Department of Psychiatry, [2]IDEA Lab, Department of Radiology and BRIC, [3]Department of Radiology and
Biomedical Research Imaging Center, University of North Carolina at Chapel Hill, NC 27514, USA, [4]State Key Lab of
Brain and Cognitive Sciences, University of Hong Kong, Hong Kong, Hong Kong, [5]Department of Biostatistics,
University of North Carolina, Chapel Hill, NC 27599, USA, [6]Laboratory of Neuropsychology and Laboratory of Social
Cognitive and Affective Neuroscience, University of Hong Kong and [7]Department of Brain and Cognitive
Engineering, Korea University, Seoul 02841, Republic of Korea

Address correspondence to Xiujuan Geng, Room 409, Sasson Road 5, Pok Fu Lam, University of Hong Kong, Hong Kong, Hong Kong. Email: gengx@hku.hk

Abstract

Brain structural covariance networks (SCNs) composed of regions with correlated variation are altered in neuropsychiatric
disease and change with age. Little is known about the development of SCNs in early childhood, a period of rapid cortical
growth. We investigated the development of structural and maturational covariance networks, including default, dorsal
attention, primary visual and sensorimotor networks in a longitudinal population of 118 children after birth to 2 years old and
compared them with intrinsic functional connectivity networks. We found that structural covariance of all networks exhibit
strong correlations mostly limited to their seed regions. By Age 2, default and dorsal attention structural networks are much less
distributed compared with their functional maps. The maturational covariance maps, however, revealed significant couplings
in rates of change between distributed regions, which partially recapitulate their functional networks. The structural and
maturational covariance of the primary visual and sensorimotor networks shows similar patterns to the corresponding
functional networks. Results indicate that functional networks are in place prior to structural networks, that correlated
structural patterns in adult may arise in part from coordinated cortical maturation, and that regional co-activation in functional
networks may guide and refine the maturation of SCNs over childhood development.

Key words: cortical thickness, early brain development, functional connectivity, maturational covariance, structural covariance

Significance Statement

Patterns of correlated variation in cortical thickness are altered in neuropsychiatric disease and are consistent with intrinsic functional connectivity networks. Little is known about the development of structural covariance networks in early childhood, a period of rapid cortical thickness growth. We investigated structural and maturational covariance networks in children from birth to age 2 years. Primary visual and sensorimotor networks had similar structural and functional network patterns. Structural covariance of the higher order default and dorsal attention networks are much less distributed compared with their functional networks. Results indicate that functional networks are in place prior to structural networks and indicate that coordinated functional activity in the cortex "sculpts" correlated patterns of cortical thickness over childhood development.

Introduction

Individual differences in normal cognitive function, neuropsychiatric disease risk, and illness severity result in part from

individual differences in brain structure (Pantelis et al. 2003; Kanai and Rees 2011). For brain structure components such as gray matter volume or cortical thickness, it has been demonstrated that there are structural covariance networks (SCNs) composed of regions with highly correlated variation. SCNs change with age (Chen, He, et al. 2011; Montembeault et al. 2012; Khundrakpam et al. 2013; Li, Pu, et al. 2013), are heritable (Mechelli et al. 2005; Schmitt et al. 2008) and are altered in neuropsychiatric disease (Bassett et al. 2008; He et al. 2008; Seeley et al. 2009; Bernhardt et al. 2011; Heinze et al. 2015). Recent studies indicate that SCNs in adults partially recapitulate the intrinsic functional connectivity networks estimated by resting-state functional MRI (rsfMRI) (Seeley et al. 2009; Chen, He, et al. 2011; Kelly et al. 2012; Li, Pu, et al. 2013), and anatomical networks constructed by white matter connectivity (Gong et al. 2012). Studies have also revealed that brain regions with high structural covariance in adults are often within systems responding to particular cognitive or behavioral functions (Andrews et al. 1997; Wright et al. 1999; He et al. 2007; Alexander-Bloch, Giedd, et al. 2013; Evans 2013).

There has been great interest in how SCNs develop, as this will provide important insights into the relationship of structural development to cognitive function (Riska 1986; Lerch et al. 2006), the pathophysiology of neuropsychiatric disease (Bullmore et al. 1997; Seeley et al. 2009; Heinze et al. 2014), as well as the biological meaning of the structural covariance (Riska 1986; Katz and Shatz 1996; Alexander-Bloch, Giedd, et al. 2013). Studies of SCNs estimated by gray matter intensity and cortical thickness in 5- to 18-year olds found that primary networks were well developed at early ages, while networks involving higher cognitive functions became more distributed and adult-like in later childhood (Zielinski et al. 2010; Khundrakpam et al. 2013). From late childhood to young adults, SCNs estimated by cortical thickness share similar properties as the "maturational covariance" networks (MCNs) defined by coupled developmental fluctuations between different brain regions (Alexander-Bloch, Giedd, et al. 2013; Alexander-Bloch, Raznahan, et al. 2013), and maturational covariance maps in the default network had similar spatial patterns to its resting-state functional connectivity network (rsFCN) and white matter connectivity in adults (Raznahan, Lerch, et al. 2011). Raznahan, Lerch, et al. (2011) noted that the main obstacle to study the coordination of cortical development is the slow cortical maturational rates. This is the case for late childhood and adolescence, when annual changes in cortical thickness are on the order of ±0.5% (Raznahan, Shaw, et al. 2011). In contrast, cortical development in early childhood is very rapid attaining an average thickness of 97% of adult values by age 2 years (Lyall et al. 2015) and represents an ideal time to study SCN development that may be more informative than studies at later ages when the bulk of development is over. Early childhood is also increasingly recognized as important period for cognitive development and risk for psychiatric disease, such as autism (Courchesne et al. 2007; Gilmore et al. 2010; Hazlett et al. 2011). Thus, the study of SCN development in the first 2 years of life will provide import insights into the development of these networks in a time of rapid growth. The growth trajectories of cortical structures, such as cortical gray matter volume and cortical thickness, as well as white matter tracts, vary from regions to region, exhibiting nonrandom patterns (Knickmeyer et al. 2008, 2010; Geng et al. 2012; Gilmore et al. 2012; Li, Nie, et al. 2013; Lyall et al. 2015). For example, primary and secondary sensory cortices tended to be slower growing, compared with some higher order association areas in the first 2 years (Lyall et al. 2015). Resting-state functional networks also develop rapidly in the first 2 years of life, with sensorimotor and visual networks being present shortly after birth, and default and dorsal attention networks becoming adult-like by age 2 years (Gao et al. 2009, 2013).

We aimed to characterize the developmental patterns of structural and maturational covariance of cortical thickness on several large networks in the first 2 postnatal years with rapid cortical maturational rate. With a relatively large longitudinal dataset, we examined SCNs and MCNs on several large-scale networks previously studied in older children and adults including primary networks such as sensorimotor and visual networks and high-order functional networks such as default and dorsal attention networks (Corbetta and Shulman 2002; Fox et al. 2005; Fair et al. 2008; Zielinski et al. 2010; Szczepanski et al. 2013). To further investigate whether SCNs and MCNs reflect functionally defined networks, we have reexamined and compared with the rsFCNs on a subset of the same cohort, who had the rsfMRI scans. We hypothesized that later maturing default and dorsal attention networks would have incomplete SCNs, and their maturational covariance would reflect their rsFCNs in this period of rapid cortical development; while early maturing sensorimotor and visual networks would exhibit adult patterns of structural co-variance that would reflect functional connectivity.

Materials and Methods

Subjects

The study was approved by the Institutional Review Board of the University of North Carolina (UNC) at Chapel Hill. Subjects were recruited prenatally and scanned under 3T MRI scanner after birth and at ages 1 and 2 years. Exclusion criteria were the presence of abnormalities on fetal ultrasound or major medical or psychotic illness in the mother. Additional exclusion criteria for this analysis included spending >24 h in the neonatal intensive care unit after birth, history of major medical illness, and major abnormality on MRI. Children who had successful T_1- or T_2-weighted MRI scans were included in this study. Three hundred high-quality scans are available for 118 children including 115 neonates (2–4 weeks of age), 100 one-year olds, and 82 two-year olds. Demographic information and distribution of scan availability are found in Tables 1 and 2.

Table 1 Demographic data

Gender	
Male	61
Female	57
Gestational age at birth (weeks)	39.2 ± 1.3
Gestational age at Scan 1 (weeks)	42.5 ± 1.5
Gestational age at Scan 2 (weeks)	94.1 ± 3.5
Gestational age at Scan 3 (weeks)	145.5 ± 3.2
Birth weight (g)	3449.1 ± 461.7
APGAR score (5 min) at Scan 1	8.9 ± 0.5
Maternal education (total in years)	15.2 ± 3.5

Table 2 Distributions of scan availability

Available scans	N
Neonate + 1 year + 2 year	62
Neonate + 1 year	98
Neonate + 2 year	79
1 year + 2 year	65
Neonate	118
1 year	100
2 years	82

Data Acquisition and Processing

Images were acquired on a head-only 3T scanner (Allegra, Siemens Medical Systems, Erlangen, Germany). All subjects were scanned without sedation while asleep, fitted with ear protection and with their heads secured in a vacuum fixation device. The 3D MPRAGE sequence was used for T_1-weighted MRI with the following parameters: TR = 1820 ms, inversion time = 1100 ms, echo time = 4.38 ms, flip angle = 7°, n = 144, spatial resolution = $1 \times 1 \times 1$ mm^3. T_2-weight images were obtained with a turbo-spin echo sequence with TR = 6200 ms, TE1 = 20 ms, TE2 = 119 ms, flip angle = 150°, and spatial resolution = $1.25 \times 1.25 \times 1.25$ mm^3 voxel with 0.5 mm interslice gap. A "fast" T_2 sequence was done with a 15% decreased TR, smaller image matrix, and fewer number of slices (5270 ms, 104×256 mm, 50 slices) for neonates who failed or were deemed likely to fail due to difficulty sleeping; 57 T_2 fast scans (14 singleton; 14 twins) were performed. There was no significant difference of the mean cortical thickness difference between the 2 T_2 scan sequences (P = 0.144). The rsfMRI was also acquired for a subset of 50 subjects available at neonate, 1, and 2 years old from the population using a T_2*-weighted echo planar imaging (EPI) sequence with TR = 2000 ms, TE = 32 ms, spatial resolution $4 \times 4 \times 4$ mm^3, and 150 volumes for time series images.

All scans were visually checked to exclude severe motion artifacts. Images were resampled to $1 \times 1 \times 1$ mm^3 and skull-stripped with cerebellum removed (Shi et al. 2012). To get the inner and outer boundaries of gray matter, a longitudinally guided level-set method was applied onto T_2-weighted images for neonates and T_1-weighted images for 1- and 2-year olds (Wang et al. 2013). The longitudinally guided method helped to overcome the challenges to segment neonatal images with low tissue contrast. Inner and outer cortical surfaces were constructed, and cortical thickness at each vertex was calculated as the shortest distance between the 2 surfaces using method described in Li et al. (2014). Detailed preprocessing steps can be found in Lyall et al. (2015). There were around 40 000 vertices constructed for each hemisphere.

Functional data were preprocessed using FMRIB's Software Libraries (FSL, v 4.1.9) (Smith et al. 2004; Jenkinson et al. 2012). The preprocessing steps included discarding the first 10 volumes, slice-timing correction, motion correction, and band-pass filtering (0.01–0.08 Hz). Mean signal from white matter, cerebrospinal fluid, the whole brain, and 6 motion parameters were removed using linear regression. To further reduce the effect of motion on functional connectivity measures, the global measure of signal change and frame-wise displacement (FD) were controlled to be <0.5% signal and 0.5 mm, respectively, as proposed by Power et al. (2012). A lower limit of >90 volumes remained after this "scrubbing" process was set as one of the inclusion criteria. To minimize potential biases induced by differences in brain sizes across age groups, we utilized an adaptive approach to spatial smoothing (Gao et al. 2015), applying a 4, 8.25, or 8.93 mm full width at half maximum Gaussian kernel (calculated based on the ratios of brain sizes across different age groups) to data from neonates, 1-year olds, and 2-year olds, respectively.

Structural and Maturational Covariance Analyses

To perform vertex-based analysis, individual cortical surfaces of younger age group were first warped to their corresponding older scans and then warped to a standard surface space provided by Freesurfer (Fischl and Dale 2000). The surface registration was performed using the publicly released spherical demons registration method (https://sites.google.com/site/yeoyeo02/software/sphericaldemonsrelease).

Four seed regions were selected to study the 4 networks including PCC, IPS, left calcarine sulcus/primary visual cortex, and central gyrus/primary motor cortex for default, dorsal attention, primary visual, and motor networks, respectively. The seeds were centered at the coordinates of [–5, –49, 40], [–25, –57, 46], [–10, –88, 5], and [–44, –8, 38] for the post cingulate cortex (PCC), intraparietal sulcus (IPS), calcarine fissure (BA17 primary visual cortex), and central gyrus (BA4 primary motor cortex), respectively. Seeds of each network were chosen based on the widely reported hub regions in the networks (Fox et al. 2005; Fair et al. 2008; Gu et al. 2010; Gao et al. 2013). We first drew a ball with radius of 6 mm in the 3D Talairach space, then projected the volumetric seeds onto the outer surface to get the seed patches, and manually edited the patches if they were slightly off the desired gyrus position due to projection error. As the seed of IPS falls in the sulcus, the projected surface area (424.8 ± 24.2 mm^2) is larger than the other seed areas (with mean areas of 293.8 ± 19.5, 301.0 ± 14.0, and 301.2 ± 19.2 for PCC, visual, and motor, respectively). To control the seed regions with similar areas, we re-drew a ball with radius of 5.2 mm to get the IPS surface area of 301.1 ± 18.3 mm^2. The cortical thickness of the seed region was defined by averaging thickness values within the seed region. Condition-by-covariate analyses on thickness were conducted with age and gender as covariates to estimate structural covariance between seed thickness and thickness of all other vertices at each age group in each network. Similar condition-by-covariate analyses were performed with age and gender as covariates on the thickness growth rate to estimate maturational covariance. The thickness changing rate over all cortex for the first 2 years (difference between Year 0 and Year 2 normalized by year 0), the first (difference between Year 0 and Year 1 normalized by year 0), and second year (difference between Year 1 and 2 normalized by year 1) were correlated with each seed region changing rate, with age and gender as covariates. Significant correlations were corrected for multiple comparison corrections using random field theory (Worsley et al. 1999; Chung et al. 2010), between entire cortical regions and the seed region. The vertex-based thickness difference was calculated between 2 different age groups by subtracting the corresponding thickness values on the warped surfaces. The growth rate between Time 1 and Time 2 was then calculated by taking the thickness difference between 2 time points then divided by the thickness of the first time point.

Functional Connectivity Analyses

To compute functional connectivity map of each network, average time series were calculated from each seed region of each individual subject and correlated with all voxels in the whole brain. The correlation coefficients were Fisher-Z transformed. Two-tailed t-test was performed for each voxel to determine whether it is significantly different from 0 ($P < 0.05$ after false discovery rate [FDR] correction; cluster size >10 voxels). Details can be found in Gao et al. (2013).

Maturational Covariance Between Homologous Regions and Gender Effect

To get the homologous vertices, the left hemisphere was warped into the right hemisphere in the standard space. We computed thickness growth rate correlations between each vertex in 1 hemisphere with the growth rate in its contralateral homolog to derive a distribution of around 40 000 correlation coefficients. We randomly sampled 40 000 contralateral vertex–vertex pairings to form around 40 000 correlation coefficients and compared the mean of these 2 distributions using Mann–-Whitney U test.

Results

We used cortical thickness, a more direct measure of cortical morphometry with subvoxel precision, to estimate the structural and maturational covariance (Prothero and Sundsten 1984; Van Essen et al. 1998; Fischl and Dale 2000). We first computed the vertex-based mean thickness of 3 age groups: after birth, at 1-year, and 2-year old; and the vertex-based mean thickness growth rate from neonate to Year 1, from Year 1 to Year 2, and from neonate to Year 2. Seed-based analyses were then conducted to map the SCN and MCN across all 3 age groups and ranges of 4 distinct networks including default, dorsal attention, primary visual, and sensorimotor networks. We also performed the homologous test of structural covariance and maturational coupling on each vertex over the entire cortex and the gender test of the cortical thickness at each age group and the developmental rate in each age range. FCNs of all 4 networks were also estimated.

Mean Thickness and Thickness Growth Rate

The mean thickness over whole cortex is 2.026 ± 0.080 mm at approximately 3 weeks, 2.611 ± 0.0726 and 2.704 ± 0.0690 mm at 1- and 2-year olds. The vertex-based cortical thickness map (Fig. 1a–c) shows that the primary visual and sensorimotor cortices always have thinner thickness compared with the average thickness across the 3 age groups. The temporal pole, medial frontal/prefrontal, and insular cortices have higher thickness in neonates; these regions together with the bilateral temporal cortex show higher thickness in the first and second years of age.

The average thickness change in the first 2 years is $34.51 \pm 6.08\%$; the thickness change in the first year is $30.43 \pm 5.86\%$; and the change in the second year is $4.29 \pm 1.77\%$. There is regionally heterogeneous growth of cortical thickness. In the first 2 years, insular cortex showed higher thickness changes, followed by medial frontal and temporal cortices compared with the average cortical thickness change; and sensorimotor and visual cortices show slower thickness changes (Fig. 1d–f). Yet, the first and

second year have different growing patterns. The first year has similar pattern as the first 2 years. In the second year, the sensorimotor and fusiform regions show faster growing rate, while the frontal and temporal cortices have slower growing rate. The patterns of the vertex-based average thickness maps and the thickness change maps show similar pattern as reported in our previous ROI-based study (Lyall et al. 2015).

Structural Covariance, Maturational Coupling, and Intrinsic Functional Connectivity Networks

We specifically chose the following cortical regions as seeds to study the corresponding 4 networks: PCC, IPS, left primary visual cortex (Vis), and left primary motor cortex (Motor), for default, dorsal attention, primary visual, and sensorimotor networks, respectively. For the calculation of the covariance maps, we have limited the subjects to the ones with the mean measures (thickness for SC maps and thickness changing rate for MC maps) within 2 standard deviations, so that the regional structural and maturational couplings are not dominated by the overall thickness or maturational rates across each subject.

Significant structural correlation maps of the 4 networks are shown in (a–c) of Figures 2, 3, 4, and 5. The default network shows correlation patterns mostly limited to the seed, posterior and occipital regions at birth, Age 1 and Age 2. The SCNs at Age 1 showed small regions in right temporal and right prefrontal areas, and the SCNs at Age 2 also include small patches in the temporal cortex and mPFC. The dorsal attention network has correlation patterns mostly limited to seed and posterior cortical regions at birth, Age 1, and Age 2. At Age 1, the SCN of IPS showed small regions in premotor and frontal eye field (FEF). The primary visual network seed has significant correlations with mainly medial occipital cortex in each age group. And the sensorimotor network seed shows significant correlations with mainly pre- and postcentral gyrus in each age group.

Significant maturational correlations are shown in (d–f) of Figures 2–5. The thickness growth rate in the first 2 years of
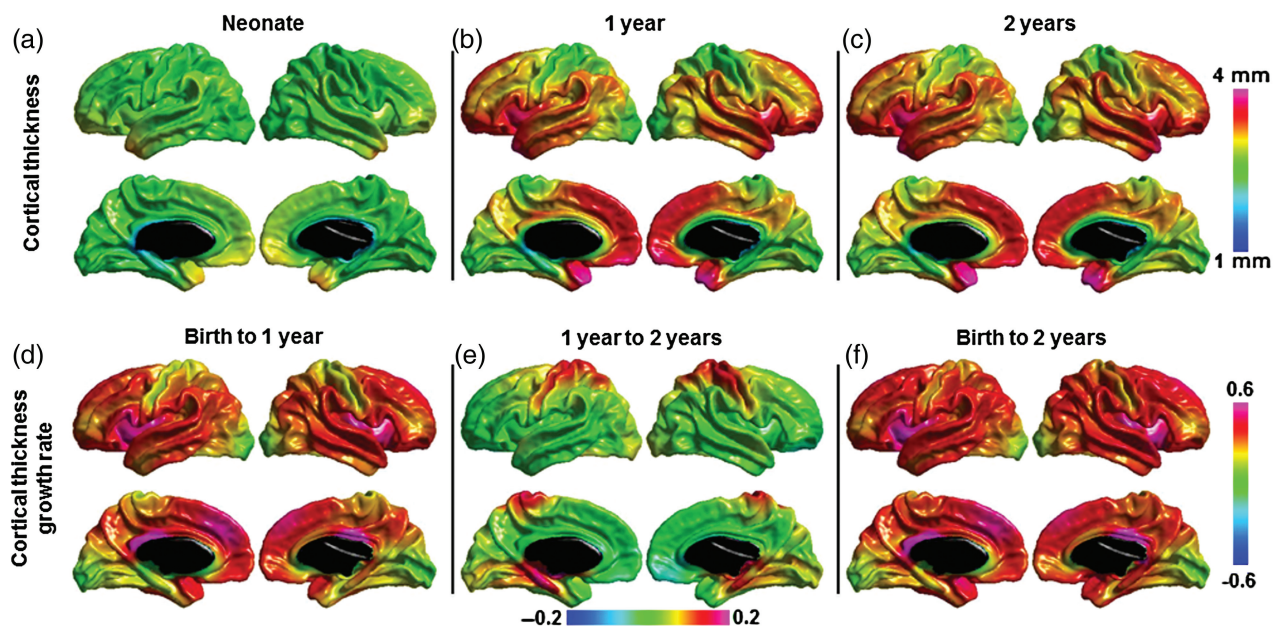

Figure 1. Mean cortical thickness and cortical thickness growth in the first 2 years of life. Note: (e) has different min/max values compared with (d) and (f) to better show the contrast of growth rate.
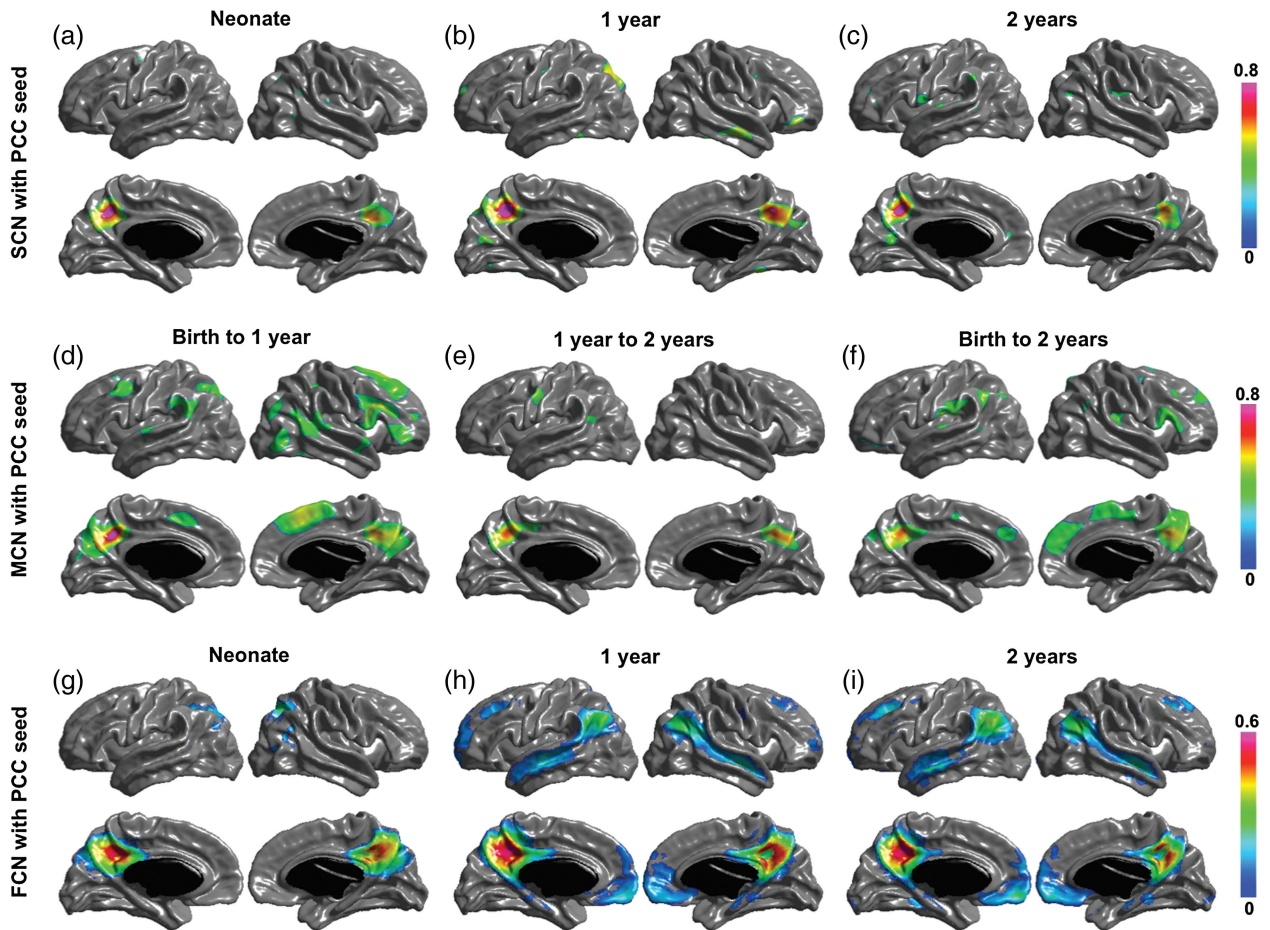
Figure 2. SCN (*a–c*), MCN (*d–f*), and FCN (*g–i*) with posterior cingulate cortex (PCC) as seed region. Correlation coefficients are shown for only significant correlated regions.

PCC seed is significantly correlated with the growth of medial frontal and prefrontal cortices, parietotemporal junction and right lateral inferior frontal gyrus (IFG) are most correlated with that of PCC seed. In the first year, the PCC seed MCN shows similar patterns as that in the first 2 years with 2 extra regions of right temporal and left frontal cortices significantly coupled with PCC seed. The 2-year MCN of IPS seed shows significant correlations in bilateral FEFs (BA6) and right IFG (BA44). The first-year MCN has similar patterns with slightly wider spread-out of each region. The maturational rate of the primary visual seed was correlated with local occipital regions and primary motor regions from birth to 1 year and was correlated with only occipital regions from 1 year to 2 years, and from birth to 2 years. The primary motor seed was correlated with the pre- and postmotor cortices, supplementary motor area, and the lateral occipital regions from birth to 1 year, and from birth to 2 years; only the surrounding primary motor regions show correlations from 1 year to 2 years.

Significant functional networks are shown in (*g–i*) of Figures 2–5. For the default FCN, at neonate, only localized regions in parietal cortex show correlations with PCC seed; starting from 1-year old, medial prefrontal cortex (mPFC), bilateral temporal cortex, bilateral inferior parietal cortex (IPL) or supramarginal gyrus (SMG), and medial temporal (hippocampus/parahippocampus) show significant connectivity with PCC. For dorsal attention network, the correlation maps start from localized diffused blobs at neonate and become to more distribute at 1-year and 2-year olds, including bilateral anterior prefrontal cortex, FEFs, and inferior/middle

temporal cortex correlated with IPS seed. The primary visual functional network shows connections mainly in occipital cortex at neonate, 1 year and 2 years, where the pattern is more diffused including small regions extended to parietal cortex at neonate. The primary motor functional network shows more diffused connections at neonate, and more spatialized connections at 1 year and 2 years, where the 2 year network also include small scattered regions in cuneus.

Figure 6 shows the regions of overlap between the maturational and functional networks for each seed. Both PCC and IPS maturational and functional networks show distributed overlapping regions in ages after the neonatal period. The PCC MCN in the first year overlaps with the FCNs at 1 and 2 years in bilateral parietotemporal junction, right temporal and medial frontal regions; and the PCC MCN from neonate to year 2 is overlapped with the FCNs at 1 and 2 years in bilateral parietotemporal junction and mPFC. The MCN of the IPS seed from neonate to Year 1 is overlapped with the FCN in Year 2 in right FEF, and the MCN of the IPS seed from neonate to Year 2 is overlapped with the FCN in Year 2 in left inferior temporal cortex and FEF. For the visual and motor seeds, the overlap between MCNs and FCNs is mostly surrounding the seeds, except for the motor MCN in the first year, which overlaps in the supplementary motor area (SMA) with the FCN in neonates and with the SMA and medial occipital regions with the FCN at Year 2. The quantitative overlapping measures (number of overlapping vertices) between the maturational networks and the structural and functional networks for each seed
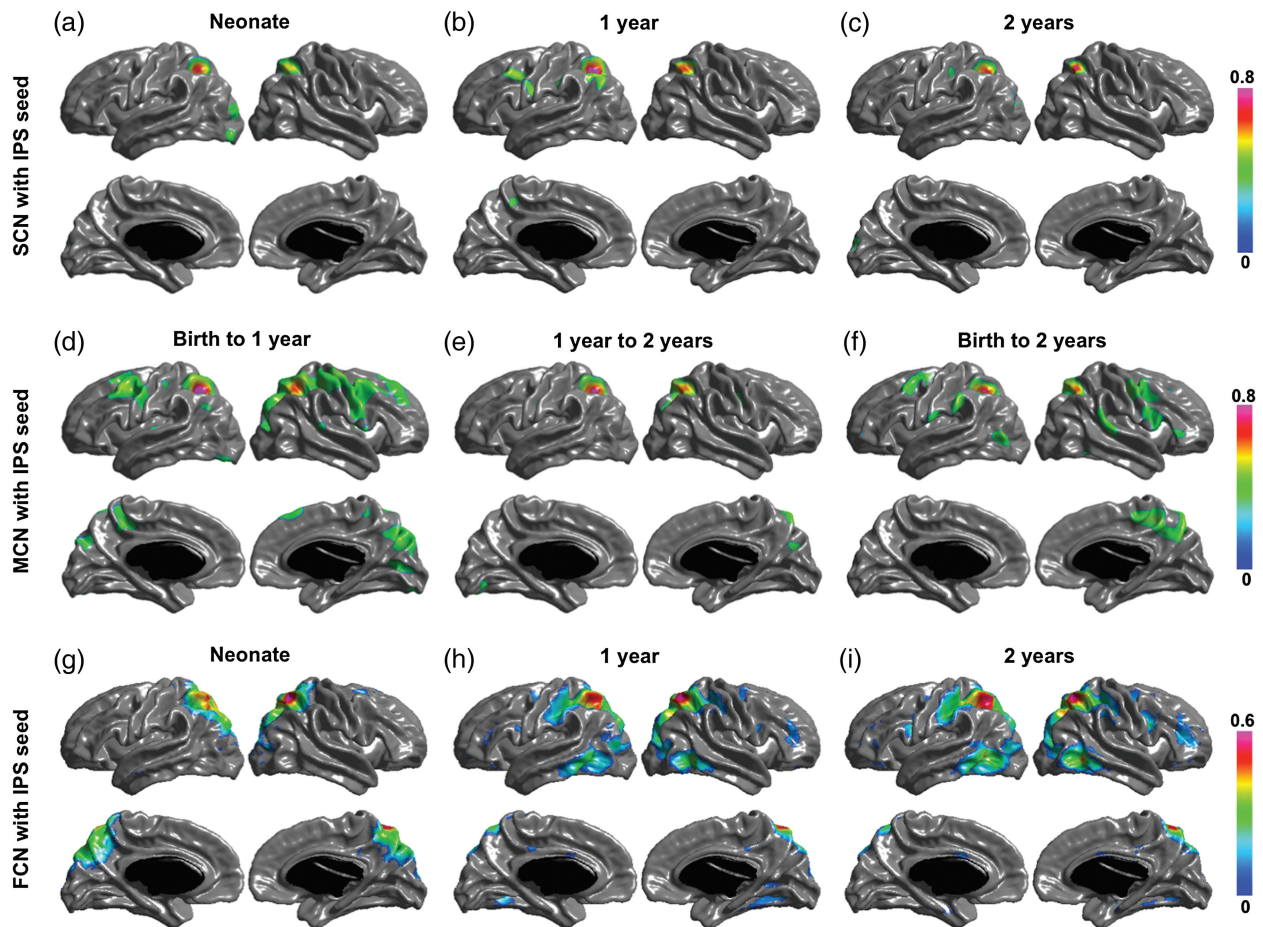
Figure 3. SCN (*a–c*), MCN (*d–f*), and FCN (*g–i*) with IPS as seed region. Correlation coefficients are shown for only significant correlated regions.

are presented in Tables 3–6. The overlap between the MCNs and the corresponding FCNs are larger compared with that between the MCNs and the corresponding SCNs, mainly due to the distributed patterns of the PCC and IPS FCNs in contrast to their isolated SCNs, as well as the slightly wider spread of the visual and motor FCNs compared with their SCNs. Table 7 shows the overlapping measures between PCC and IPS MCNs. By comparing Tables 3, 4, and 7, we found that even though the PCC and IPS MCNs are distributed, they overlap more with their corresponding FCNs compared with the overlaps of MCNs of other seeds.

Maturational Covariance Between Homologous Regions and Gender Effect

Results from Mann–Whitney *U* test show that the correlation in thickness and thickness growth between homologous vertices was significantly higher than that between nonhomologous pairings. Gender effect has been tested in the cortical thickness at each age group, and thickness growth rate in the first 2 years, the first and second year, and no gender effect on cortical thickness nor the maturation rate was found in each case.

Discussion

We have analyzed the structural covariance and maturational coupling of 4 networks in the first 2 years of life, a period of very rapid cortical thickness development, and found important

contrasts to patterns described in older children and adolescents. From birth to age 2 years, structural covariance of all networks exhibits strong correlations mostly limited to their seed and surrounding regions. By age 2 years, default and dorsal attention SCNs are much less distributed compared with their rsFCNs. The maturational covariance maps, however, revealed significant couplings between distributed regions. Moreover, the patterns of most correlated regions in the default and dorsal attention MCNs partially recapitulate the functional networks defined by rsFC. The structural covariance and maturational coupling of the primary visual and sensorimotor networks show similar patterns to the corresponding FCNs.

Our findings of localized default and dorsal attention SCNs and distributed rsFCNs in the first 2 years indicate that their functional networks are in place much earlier than their SCNs. Dissociable large-scale networks, task negative or default network, and task positive or dorsal attention network have been revealed by rsfMRI studies (Raichle et al. 2001; Fox et al. 2006) and are shown to be temporally anti-correlated with each other (Fox et al. 2005). Our previous study of these 2 networks using rsFC in early childhood shows that both networks start from an isolated region in neonates, and evolve to distributed networks at 1-year old and are further enhanced at 2 years old (Gao et al. 2009, 2013). In this study, we confirmed similar developmental patterns of their rsFCNs. The expansion of the attention network from in the isolated region to the distributed regions including FEF and IPS in the first year may reflect the emergence and
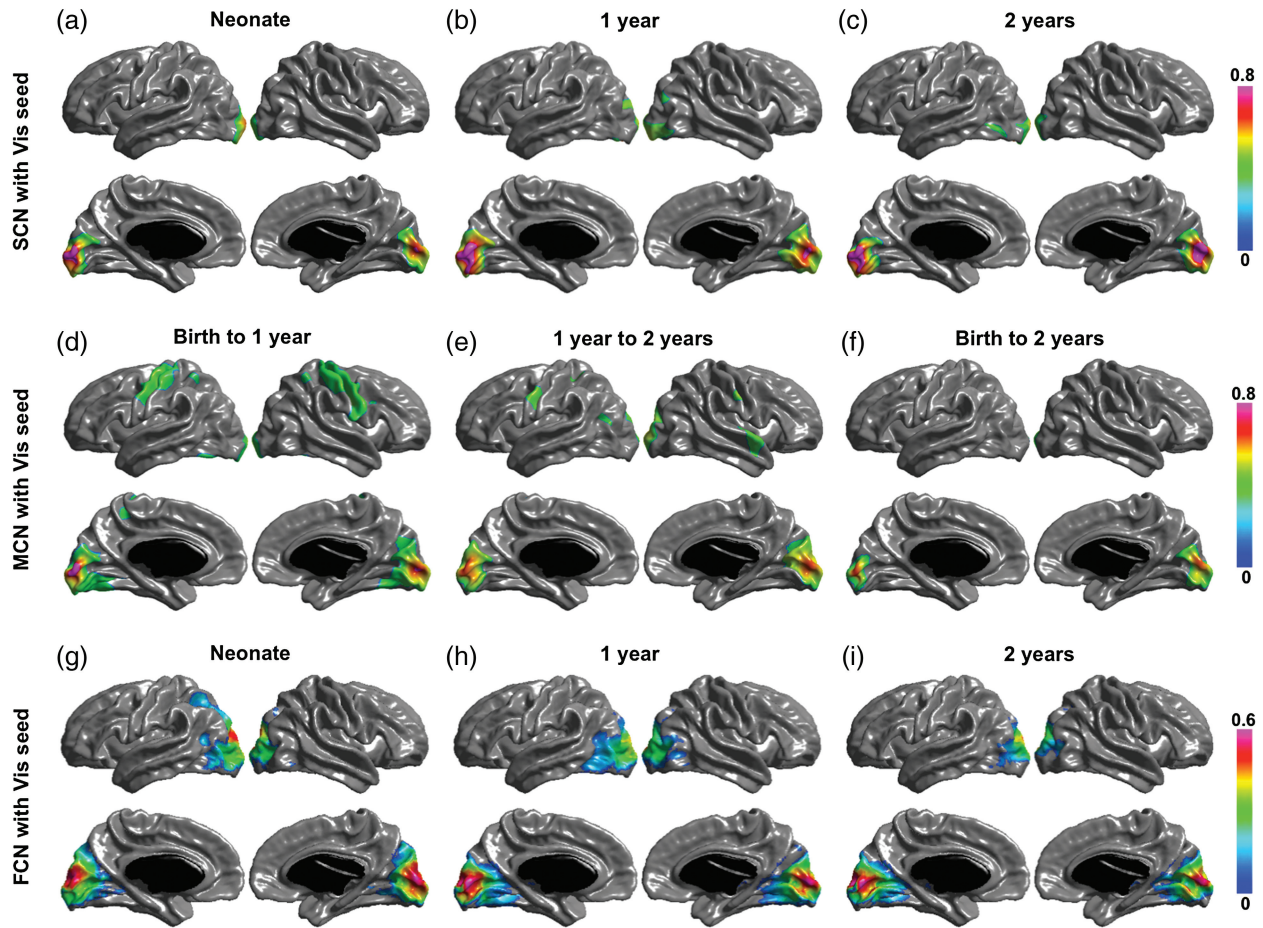
Figure 4. SCN (*a–c*), MCN (*d–f*), and FCN (*g–i*) with primary visual cortex (Vis) as seed region. Correlation coefficients are shown for only significant correlated regions.

development of some attentional functions during the first years of life, such as the ability to sustain a vigilant state was present in infants younger than 1-year old (Colombo 2001). In contrast, their SCNs show localized patterns throughout the first 2 years of life. The isolated default SCN in early age is in line with Zielinski et al.'s (2010) work, which reported that the structural covariance measured by gray matter volume had localized patterns in childhood, and that younger age group of 4.9–7.8 years showed more localized topology compared with older age group from 8.5 to 14.2 years. As a signature of the "resting" brain under passive or undirected mental state (Raichle et al. 2001), default network constructed by structural covariance has similar patterns compared with that estimated by rsFC in adults (Seeley et al. 2009; Chen, He, et al. 2011). All evidence above suggests that the distributed patterns of the higher order SCNs may emerge in later ages, whereas their rsFCNs are in place as early as Age 2.

Unlike the completely different patterns of the higher order networks, the SCN and rsFCN of primary visual and sensorimotor networks show similar spatial patterns. For these networks, their SCNs were very similar to that observed in older children and adults, suggesting that the SCN is established early in life. The primary visual SCN included mainly medial occipital cortex, and the sensorimotor SCN showed significant correlations with pre- and postcentral gyrus in each age group. The primary visual rsFCN showed connected regions mainly in occipital cortex in the first 2 years, with a slightly more diffused pattern extending to parietal cortex at neonate. The primary sensorimotor rsFCN

also had more diffused connections at neonate followed by more restricted connections at 1 and 2 years, and the main connections are overlapped with its SCN. The primary networks show different properties compared with the higher order networks, indicating that brain networks develop following functional specific patterns in the early years of life.

In contrast to the isolated SCNs, our study revealed distributed MCNs in the first 2 years of life, and the MCNs partially overlapped with the corresponding rsFCNs, though not identical to the pattern as shown in later ages (Raznahan, Lerch, et al. 2011). For the default and dorsal attention networks, the MCN from birth to Age 1 was consistent with the expanding FCN at Age 1. From birth to Age 1, default functional network expanded to include medial prefrontal/frontal, parietotemporal, temporal, and lateral superior prefrontal regions. Each of these regions, except for the medial and lateral prefrontal regions, overlapped with the MCN from birth to Age 1. In a similar way, from birth to Age 1, the dorsal attention functional network expanded to include inferior temporal, dorsolateral prefrontal, and parietal regions, as well as the inferior temporal and dorsal frontal cortices that were part of the MCN. There were also many regions of the MCN for both default and dorsal attention networks that did not correspond to expanded regions of the corresponding functional networks. While there was not much change in the structural and functional networks, the primary visual and sensorimotor MCNs showed more distributed patterns from birth to Age 2. The primary visual MCNs of the first and second year
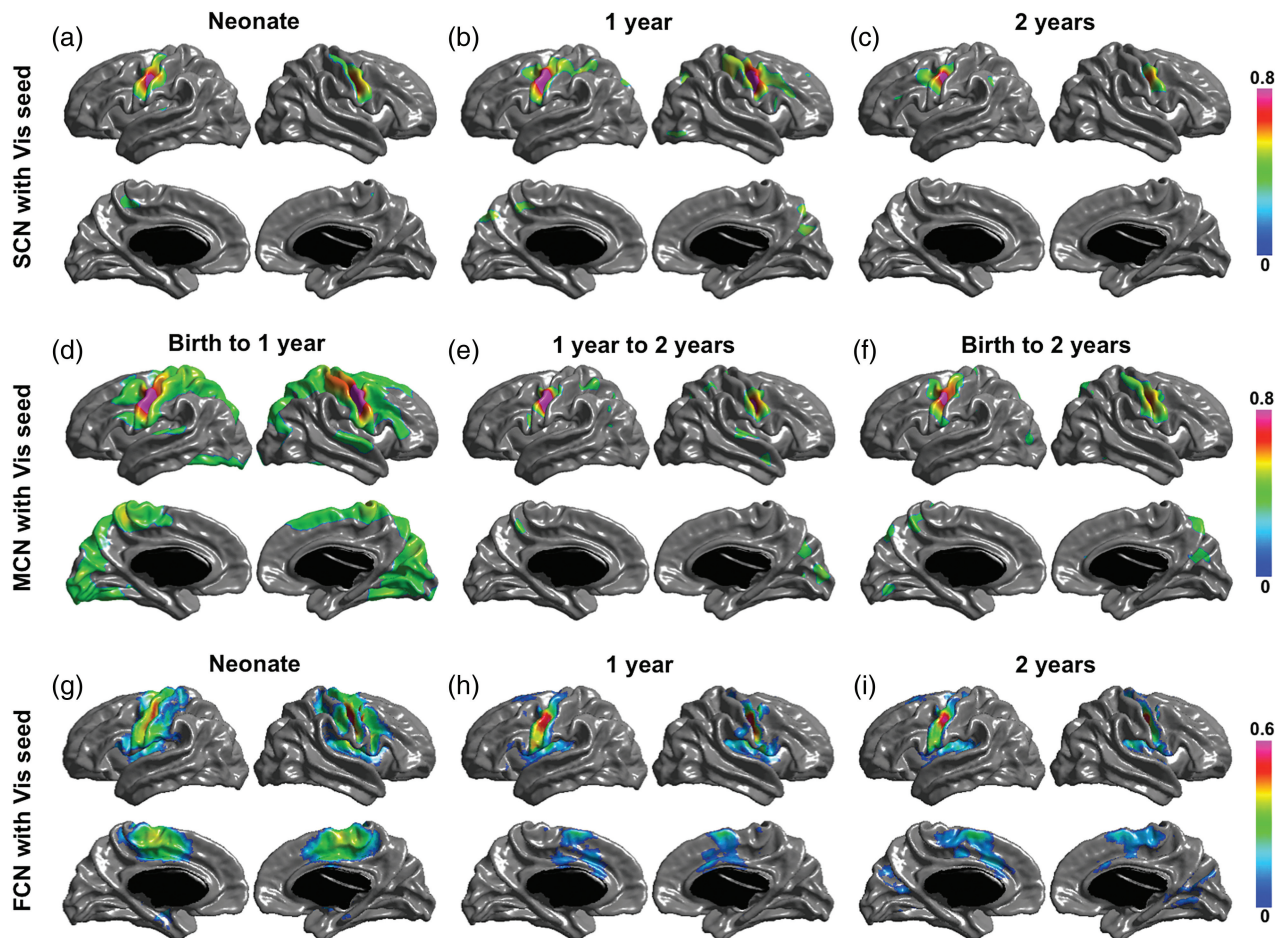
Figure 5. SCN (*a–c*), MCN (*d–f*), and FCN (*g–i*) with primary motor cortex (Motor) as seed region. Correlation coefficients are shown for only significant correlated regions.

included sensorimotor cortex. The sensorimotor MCN included a broader region of the sensorimotor cortex and visual cortex, although its functional network became more refined from birth to Age 2 years.

Thus, coordinated functional activity is associated with several patterns of relationship with the MCN—1) regions of the MCN with clear associations with expanding FCNs, 2) regions of the MCN associated with no change in the corresponding FCN, 3) regions of FCN development with no corresponding regions in the MCN, and 4) for the sensorimotor network, regions of the MCN that corresponded with a loss of participation in the FCN. The relationship of MCN and FCN in the first 2 years of life are complex and likely dependent on the specific network and the overall stage of maturation (primary vs. higher order), as well as overall patterns of very rapid growth that may result in MCNs that do not correspond with FCNs.

The mass growth of cortical thickness from birth to Age 2 years does not predict the development of the SCNs either. While there is significant growth, overall adult patterns are present at birth (Lyall et al. 2015), and there is no apparent change in the SCN for any of the networks studied from birth to Age 2 years. Further study is needed, but it is apparent that the close relationship between SCN, MCN, and FCN described in older childhood does not exist in early childhood. It has recently been shown that amygdala functional connectivity is abnormal in neonates with prenatal maternal depression (Qiu et al. 2015), indicating that functional network abnormalities associated with

psychiatric disorders are present at birth, before the bulk of cortical thickness and surface area growth. This suggests that abnormal functional networks are present very early and that abnormal SCN associated with psychiatric illness develop secondary to the abnormal functional network.

Little is known about the biological relationships between networks defined by different measures such as rsFC, structural, and maturational covariance. Several studies suggested that SCNs reflect shared recruitment or common neurodevelopmental effects within functionally coactive regions (Seeley et al. 2009; Zielinski et al. 2010; Alexander-Bloch, Giedd, et al. 2013; Clos et al. 2014). Our findings support this speculation. There are different topological patterns of maturational coupling and structural covariance of higher order networks including default and dorsal attention networks in the first years of life. Starting with isolated structural networks, their MCNs exhibit distributed patterns partially overlapped with the rsFCNs by age 2 years. And the functional networks by Age 2 already exhibit similar patterns as observed in adults, indicating a delayed onset of the structural networks. On the other hand, Alexander-Bloch, Raznahan et al. (2013) revealed that in children and adolescence, the maturational and structural covariance maps are highly correlated across brain regions, and their networks are topologically similar. Moreover, the structural networks also reflect with functional networks in adults (Seeley et al. 2009; Gong et al. 2012; Clos et al. 2014). All above suggest that the distributed structural covariance in adults may result from synchronized current and earlier maturation in
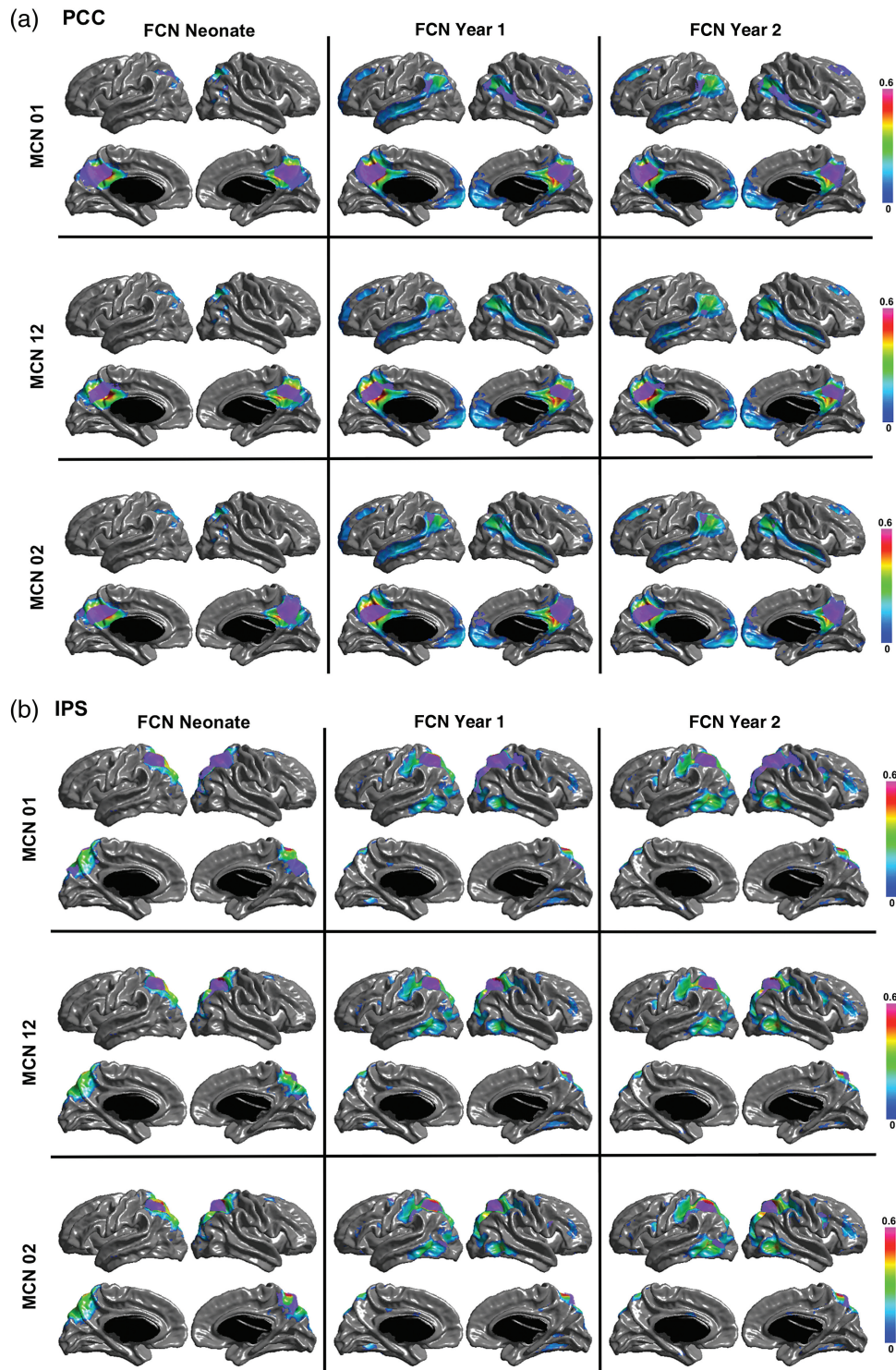
Figure 6. The overlapping regions between the MCN and FCN for each seed. The purple color patches show the overlaps between the networks for the (*a*) PCC, (*b*) IPS, (*c*) Visual, and (*d*) Motor seeds.

regions that co-activate serving for some specific functional processing.

Recent adult studies using a twin design have found that cortical thickness has up to 12 regional clusters of genetic correlations that were bilateral symmetric (Rimol et al. 2010; Chen et al. 2013), which are consistent with genetic regionalization in rodents (Chen, Panizzon, et al. 2011). While genetic correlations

of cortical regionalization studies have not been performed at young ages, different patterns of SCN and MCN in early life compared with adulthood suggest that patterns of genetic regionalization are not consistent with SCN or MCN in early childhood.

We did not find gender effect of the early development of SCNs and MCNs. Several studies revealed some cognitive functions including speech and salience maturing earlier in females
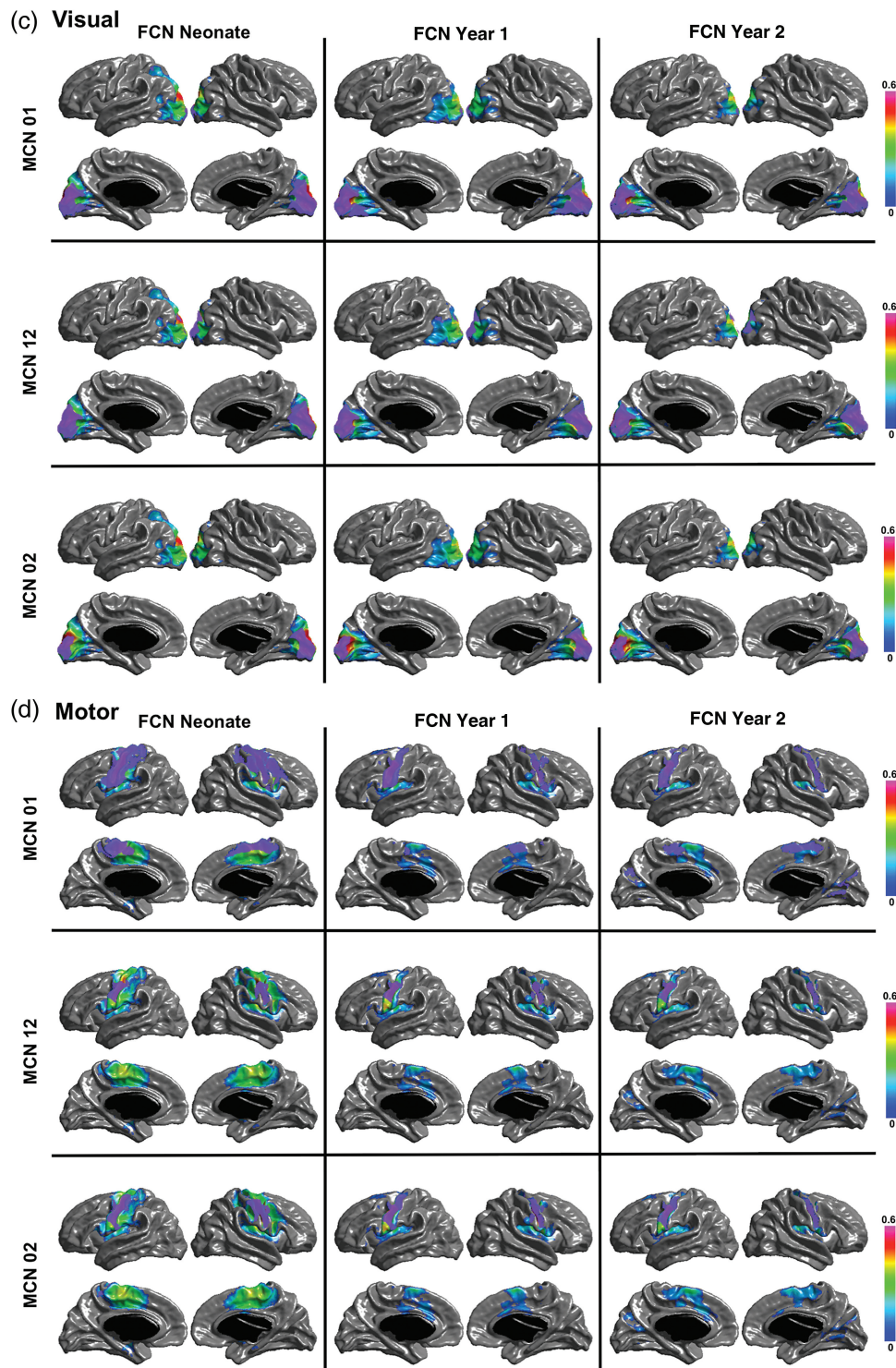
Figure 6 Continued

(Lenroot et al. 2007; Blakemore 2008). We therefore postulate that the gender maturational differences may not exist in early brain development but appear until late childhood or early adolescence.

One limitation of the current study lies in the well-known fact that the "white matter" tissue before 6 months of old represents different image contrast compared with later ages, and therefore,

the cortical thickness estimation of neonate might be less consistent with that of 1-year old compared with the estimation between 1 year and 2 years old. To minimize the possible biased estimation of cortical thickness caused by the biological "inconsistency," in our work, we utilized the longitudinal information to guide the early brain tissue segmentation to improve the consistency. Although the "disjunction" of the thickness calculation at

Table 3 Similarity measures calculated by the number of overlapping vertices between MC and FC maps, overlap between MC and SC, FC maps of the PCC seed

PCC	SC at Neo	SC at 1 year	SC at 2 years	FC at Neo	FC at 1 year	FC at 2 years
MC of 0–1year	1161	1968	1228	3237	3926	3713
MC of 1–2 years	874	1179	970	1439	1660	1521
MC of 0–2 years	937	1253	1189	2514	2837	3007

Table 4 Similarity measures calculated by the number of overlapping vertices between MC and FC maps, overlap between MC and SC, FC maps of the IPS seed

IPS 0.3	SC at Neo	SC at 1 year	SC at 2 years	FC at Neo	FC at 1 year	FC at 2 years
MC of 0–1 year	1167	1520	1218	3981	4533	4793
MC of 1–2 years	1071	1274	1141	2390	2363	2349
MC of 0–2 years	937	1251	1062	2464	2742	2873

Table 5 Similarity measures calculated by the number of overlapping vertices between MC and FC maps, overlap between MC and SC, FC maps of the Visual seed

Visual	SC at Neo	SC at 1 year	SC at 2 years	FC at Neo	FC at 1 year	FC at 2 years
MC of 0–1 year	2085	2787	2608	2990	3639	3123
MC of 1–2 years	1737	2073	1839	2948	2924	2754
MC of 0–2 years	1346	1415	1417	1512	1490	1381

Table 6 Similarity measures calculated by the number of overlapping vertices between MC and FC maps, overlap between MC and SC, FC maps of the Motor seed

Motor	SC at Neo	SC at 1 year	SC at 2 years	FC at Neo	FC at 1 year	FC at 2 years
MC of 0–1 year	3506	5460	2161	11 245	4898	5820
MC of 1–2 years	1964	2398	1595	2660	2056	2022
MC of 0–2 years	3075	3587	1890	4310	3202	3060

Table 7 Similarity measures calculated by the number of overlapping vertices between MC and FC maps, overlap between the PCC MC maps and the IPS MC maps

0.3	IPS 0–1 year	IPS 1–2 years	IPS 0–2 years
PCC 0–1 year	2614	422	1966
PCC 1–2 years	650	89	425
PCC 0–2 years	467	284	1363

neonate and 1 and 2 years exists, the surface extraction and therefore the thickness calculation of neonatal thickness depend on the local distributions of image intensities, meaning that if the contrasts in 2 distributed regions follow similar patterns, then the thickness estimated in the 2 regions will have similar values even the absolute values may not be accurate. Therefore, it is reasonable to assume that the covariance maps may be affected less by the inconsistent contrasts between 2 age groups.

Together with findings from studies in older populations, our finding of isolated SCNs and distributed MCNs that partially overlap with rsFCNs suggests that structural networks develop later than functional networks and that the region-specific co-activation of functional networks may guide the maturation of SCNs and refine SCNs over many years during childhood development. Therefore, the altered patterns of cortical thickness observed in many neurodevelopmental and neuropsychiatric disorders may reflect abnormal functional connectivity that is present early in childhood and "sculpting" later developing SCNs. Future studies, such as directly testing the "sculpting" model by conjunction analyses between the FCNs and SCNs over time, will need to better delineate the relationships between developing functional and structural networks in both typically developing and high-risk children.

Funding

Notes

Conflict of Interest: None declared.

References

Alexander-Bloch A, Giedd JN, Bullmore ET. 2013. Imaging structural co-variance between human brain regions. Nat Rev Neurosci. 14:322–336.
Alexander-Bloch A, Raznahan A, Bullmore ET, Giedd J. 2013. The convergence of maturational change and structural covariance in human cortical networks. J Neurosci. 33:2889–2899.

Andrews TJ, Halpern SD, Purves D. 1997. Correlated size variations in human visual cortex, lateral geniculate nucleus, and optic tract. J Neurosci. 17:2859–2868.

Bassett DS, Bullmore ET, Verchinski BA, Mattay VS, Weinberger DR, Meyer-Lindenberg A. 2008. Hierarchical organization of human cortical networks in health and schizophrenia. J Neurosci. 28:9239–9248.

Bernhardt BC, Chen Z, He Y, Evans AC, Bernasconi N. 2011. Graph-theoretical analysis reveals disrupted small-world organization of cortical thickness correlation networks in temporal lobe epilepsy. Cereb Cortex. 21:2147–2157.

Blakemore SJ. 2008. The social brain in adolescence. Nat Rev Neurosci. 9:267–277.

Bullmore ET, Frangou S, Murray RM. 1997. The dysplastic net hypothesis: an integration of developmental and dysconnectivity theories of schizophrenia. Schizophr Res. 28:143–156.

Chen CH, Fiecas M, Gutierrez ED, Panizzon MS, Eyler LT, Vuoksimaa E, Thompson WK, Fennema-Notestine C, Hagler DJ Jr, Jernigan TL, et al. 2013. Genetic topography of brain morphology. Proc Natl Acad Sci U S A. 110:17089–17094.

Chen CH, Panizzon MS, Eyler LT, Jernigan TL, Thompson W, Fennema-Notestine C, Jak AJ, Neale MC, Franz CE, Hamza S, et al. 2011. Genetic influences on cortical regionalization in the human brain. Neuron. 72:537–544.

Chen ZJ, He Y, Rosa-Neto P, Gong GL, Evans AC. 2011. Age-related alterations in the modular organization of structural cortical network by using cortical thickness from MRI. Neuroimage. 56:235–245.

Chung MK, Worsley KJ, Nacewicz BM, Dalton KM, Davidson RJ. 2010. General multivariate linear modeling of surface shapes using SurfStat. Neuroimage. 53:491–505.

Clos M, Rottschy C, Laird AR, Fox PT, Eickhoff SB. 2014. Comparison of structural covariance with functional connectivity approaches exemplified by an investigation of the left anterior insula. Neuroimage. 99:269–280.

Colombo J. 2001. The development of visual attention in infancy. Annu Rev Psychol. 52:337–367.

Corbetta M, Shulman GL. 2002. Control of goal-directed and stimulus-driven attention in the brain. Nat Rev Neurosci. 3:201–215.

Courchesne E, Pierce K, Schumann CM, Redcay E, Buckwalter JA, Kennedy DP, Morgan J. 2007. Mapping early brain development in autism. Neuron. 56:399–413.

Evans AC. 2013. Networks of anatomical covariance. Neuroimage. 80:489–504.

Fair DA, Cohen AL, Dosenbach NU, Church JA, Miezin FM, Barch DM, Raichle ME, Petersen SE, Schlaggar BL. 2008. The maturing architecture of the brain's default network. Proc Natl Acad Sci U S A. 105:4028–4032.

Fischl B, Dale AM. 2000. Measuring the thickness of the human cerebral cortex from magnetic resonance images. Proc Natl Acad Sci U S A. 97:11050–11055.

Fox MD, Corbetta M, Snyder AZ, Vincent JL, Raichle ME. 2006. Spontaneous neuronal activity distinguishes human dorsal and ventral attention systems. Proc Natl Acad Sci U S A. 103:10046–10051.

Fox MD, Snyder AZ, Vincent JL, Corbetta M, Van Essen DC, Raichle ME. 2005. The human brain is intrinsically organized into dynamic, anticorrelated functional networks. Proc Natl Acad Sci U S A. 102:9673–9678.

Gao W, Alcauter S, Elton A, Hernandez-Castillo C, Smith J, Ramirez J, Lin W. 2015. Network development during the first year: relative sequence and socioeconomic correlations. Cereb Cortex. 25:2919–2928.

Gao W, Gilmore JH, Shen DG, Smith JK, Zhu HT, Lin WL. 2013. The synchronization within and interaction between the default and dorsal attention networks in early infancy. Cereb Cortex. 23:594–603.

Gao W, Zhu H, Giovanello KS, Smith JK, Shen D, Gilmore JH, Lin W. 2009. Evidence on the emergence of the brain's default network from 2-week-old to 2-year-old healthy pediatric subjects. Proc Natl Acad Sci U S A. 106:6790–6795.

Geng X, Gouttard S, Sharma A, Cu HB, Styner M, Lin WL, Gerig G, Gilmore JH. 2012. Quantitative tract-based white matter development from birth to age 2 years. Neuroimage. 61:542–557.

Gilmore JH, Kang C, Evans DD, Wolfe HM, Smith JK, Lieberman JA, Lin W, Hamer RM, Styner M, Gerig G. 2010. Prenatal and neonatal brain structure and white matter maturation in children at high risk for schizophrenia. Am J Psychiatry. 167:1083–1091.

Gilmore JH, Shi F, Woolson SL, Knickmeyer RC, Short SJ, Lin WL, Zhu HT, Hamer RM, Styner M, Shen DG. 2012. Longitudinal development of cortical and subcortical gray matter from birth to 2 years. Cereb Cortex. 22:2478–2485.

Gong GL, He Y, Chen ZJ, Evans AC. 2012. Convergence and divergence of thickness correlations with diffusion connections across the human cerebral cortex. Neuroimage. 59:1239–1248.

Gu H, Salmeron BJ, Ross TJ, Geng X, Zhan W, Stein EA, Yang Y. 2010. Mesocorticolimbic circuits are impaired in chronic cocaine users as demonstrated by resting-state functional connectivity. Neuroimage. 53:593–601.

Hazlett HC, Poe MD, Gerig G, Styner M, Chappell C, Smith RG, Vachet C, Piven J. 2011. Early brain overgrowth in autism associated with an increase in cortical surface area before age 2 years. Arch Gen Psychiatry. 68:467–476.

He Y, Chen ZJ, Evans AC. 2007. Small-world anatomical networks in the human brain revealed by cortical thickness from MRI. Cereb Cortex. 17:2407–2419.

He Y, Chen Z, Evans A. 2008. Structural insights into aberrant topological patterns of large-scale cortical networks in Alzheimer's Disease. J Neurosci. 28:4756–4766.

Heinze K, Reniers RL, Nelson B, Yung AR, Lin A, Harrison BJ, Pantelis C, Velakoulis D, McGorry PD, Wood SJ. 2015. Discrete alterations of brain network structural covariance in individuals at ultra-high risk for psychosis. Biol Psychiatry. 77:989–996.

Jenkinson M, Beckmann CF, Behrens TE, Woolrich MW, Smith SM. 2012. Fsl. Neuroimage. 62:782–790.

Kanai R, Rees G. 2011. The structural basis of inter-individual differences in human behaviour and cognition. Nat Rev Neurosci. 12:231–242.

Katz LC, Shatz CJ. 1996. Synaptic activity and the construction of cortical circuits. Science. 274:1133–1138.

Kelly C, Toro R, Di Martino A, Cox CL, Bellec P, Castellanos FX, Milham MP. 2012. A convergent functional architecture of the insula emerges across imaging modalities. Neuroimage. 61:1129–1142.

Khundrakpam BS, Reid A, Brauer J, Carbonell F, Lewis J, Ameis S, Karama S, Lee J, Chen Z, Das S, et al. 2013. Developmental changes in organization of structural brain networks. Cereb Cortex. 23:2072–2085.

Knickmeyer RC, Gouttard S, Kang CY, Evans D, Wilber K, Smith JK, Hamer RM, Lin W, Gerig G, Gilmore JH. 2008. A structural MRI study of human brain development from birth to 2 years. J Neurosci. 28:12176–12182.

Knickmeyer RC, Styner M, Short SJ, Lubach GR, Kang C, Hamer R, Coe CL, Gilmore JH. 2010. Maturational trajectories of cortical brain development through the pubertal transition: unique species and sex differences in the monkey revealed through

structural magnetic resonance imaging. Cereb Cortex. 20:1053–1063.

Lenroot RK, Gogtay N, Greenstein DK, Wells EM, Wallace GL, Clasen LS, Blumenthal JD, Lerch J, Zijdenbos AP, Evans AC, et al. 2007. Sexual dimorphism of brain developmental trajectories during childhood and adolescence. Neuroimage. 36:1065–1073.

Lerch JP, Worsley K, Shaw WP, Greenstein DK, Lenroot RK, Giedd J, Evans AC. 2006. Mapping anatomical correlations across cerebral cortex (MACACC) using cortical thickness from MRI. Neuroimage. 31:993–1003.

Li G, Nie J, Wang L, Shi F, Gilmore JH, Lin W, Shen D. 2014. Measuring the dynamic longitudinal cortex development in infants by reconstruction of temporally consistent cortical surfaces. Neuroimage. 90:266–279.

Li G, Nie JX, Wang L, Shi F, Lin WL, Gilmore JH, Shen DG. 2013. Mapping region-specific longitudinal cortical surface expansion from birth to 2 years of age. Cereb Cortex. 23:2724–2733.

Li XW, Pu F, Fan YB, Niu HJ, Li SY, Li DY. 2013. Age-related changes in brain structural covariance networks. Front Hum Neurosci. 7:98.

Lyall AE, Shi F, Geng X, Woolson S, Li G, Wang L, Hamer RM, Shen D, Gilmore JH. 2015. Dynamic development of regional cortical thickness and surface area in early childhood. Cereb Cortex. 25:2204–2212.

Mechelli A, Friston KJ, Frackowiak RS, Price CJ. 2005. Structural covariance in the human cortex. J Neurosci. 25:8303–8310.

Montembeault M, Joubert S, Doyon J, Carrier J, Gagnon JF, Monchi O, Lungu O, Belleville S, Brambati SM. 2012. The impact of aging on gray matter structural covariance networks. Neuroimage. 63:754–759.

Pantelis C, Velakoulis D, McGorry PD, Wood SJ, Suckling J, Phillips LJ, Yung AR, Bullmore ET, Brewer W, Soulsby B, et al. 2003. Neuroanatomical abnormalities before and after onset of psychosis: a cross-sectional and longitudinal MRI comparison. Lancet. 361:281–288.

Power JD, Barnes KA, Snyder AZ, Schlaggar BL, Petersen SE. 2012. Spurious but systematic correlations in functional connectivity MRI networks arise from subject motion. Neuroimage. 59:2142–2154.

Prothero JW, Sundsten JW. 1984. Folding of the cerebral-cortex in mammals - a scaling model. Brain Behav Evolut. 24:152–167.

Qiu A, Anh TT, Li Y, Chen H, Rifkin-Graboi A, Broekman BFP, Kwek K, Saw SM, Chong YS, Gluckman PD, et al. 2015. Prenatal maternal depression alters amygdala functional connectivity in 6-month-old infants. Transl Psychiatry. 5:e508.

Raichle ME, MacLeod AM, Snyder AZ, Powers WJ, Gusnard DA, Shulman GL. 2001. A default mode of brain function. Proc Natl Acad Sci U S A. 98:676–682.

Raznahan A, Lerch JP, Lee N, Greenstein D, Wallace GL, Stockman M, Clasen L, Shaw PW, Giedd JN. 2011. Patterns of coordinated anatomical change in human cortical development: a longitudinal neuroimaging study of maturational coupling. Neuron. 72:873–884.

Raznahan A, Shaw P, Lalonde F, Stockman M, Wallace GL, Greenstein D, Clasen L, Gogtay N, Giedd JN. 2011. How does your cortex grow? J Neurosci. 31:7174–7177.

Rimol LM, Panizzon MS, Fennema-Notestine C, Eyler LT, Fischl B, Franz CE, Hagler DJ, Lyons MJ, Neale MC, Pacheco J, et al. 2010. Cortical thickness is influenced by regionally specific genetic factors. Biol Psychiatry. 67:493–499.

Riska B. 1986. Some models for development, growth, and morphometric correlation. Evolution. 40:1303–1311.

Schmitt JE, Lenroot RK, Wallace GL, Ordaz S, Taylor KN, Kabani N, Greenstein D, Lerch JP, Kendler KS, Neale MC, et al. 2008. Identification of genetically mediated cortical networks: a multivariate study of pediatric twins and siblings. Cereb Cortex. 18:1737–1747.

Seeley WW, Crawford RK, Zhou J, Miller BL, Greicius MD. 2009. Neurodegenerative diseases target large-scale human brain networks. Neuron. 62:42–52.

Shi F, Wang L, Dai Y, Gilmore JH, Lin W, Shen D. 2012. LABEL: pediatric brain extraction using learning-based meta-algorithm. Neuroimage. 62:1975–1986.

Smith SM, Jenkinson M, Woolrich MW, Beckmann CF, Behrens TE, Johansen-Berg H, Bannister PR, De Luca M, Drobnjak I, Flitney DE, et al. 2004. Advances in functional and structural MR image analysis and implementation as FSL. Neuroimage. 23(Suppl. 1):S208–S219.

Szczepanski SM, Pinsk MA, Douglas MM, Kastner S, Saalmann YB. 2013. Functional and structural architecture of the human dorsal frontoparietal attention network. Proc Natl Acad Sci U S A. 110:15806–15811.

Van Essen DC, Drury HA, Joshi S, Miller MI. 1998. Functional and structural mapping of human cerebral cortex: solutions are in the surfaces. Proc Natl Acad Sci U S A. 95:788–795.

Wang L, Shi F, Yap PT, Lin W, Gilmore JH, Shen D. 2013. Longitudinally guided level sets for consistent tissue segmentation of neonates. Hum Brain Mapp. 34:956–972.

Worsley KJ, Andermann M, Koulis T, MacDonald D, Evans AC. 1999. Detecting changes in nonisotropic images. Hum Brain Mapp. 8:98–101.

Wright IC, Ellison ZR, Sharma T, Friston KJ, Murray RM, McGuire PK. 1999. Mapping of grey matter changes in schizophrenia. Schizophr Res. 35:1–14.

Zielinski BA, Gennatas ED, Zhou JA, Seeley WW. 2010. Network-level structural covariance in the developing brain. Proc Natl Acad Sci U S A. 107:18191–18196.